Cytotoxic Effect of Nano-SiO$_2$ in Human Breast Cancer Cells *via* Modulation of EGFR Signaling Cascades

DONGHWAN JEON[1], HYUNGJOO KIM[1], KEESOO NAM[1],
SUNHWA OH[1], SEOG-HO SON[1] and INCHEOL SHIN[1,2]

[1]*Department of Life Science, and* [2]*Natural Science Institute,*
Hanyang University, Seoul, Republic of Korea

Abstract. *Background/Aim: Silica nanoparticles (nano-SiO$_2$) are widely used in many industrial areas and there is much controversy surrounding cytotoxic effects of such nanoparticles. In order to determine the toxicity and possible molecular mechanisms involved, we conducted several tests with two breast cancer cell lines, MDA-MB-231 and Hs578T. Materials and Methods: After exposure to nano-SiO$_2$, growth, apoptosis, motility of breast cancer cells were monitored. In addition, modulation of signal transduction induced by nano-SiO$_2$ was detected through western blot analysis. Results: Treatment of nano-SiO$_2$ repressed the growth of breast cancer cell lines. It also increased apoptosis and reduced cell motility. Moreover, exposure to nano-SiO$_2$ significantly disturbed the dimerization of epidermal growth factor receptor (EGFR), followed by down-regulation of its downstream cellular sarcoma kinase (c-SRC) and signal transducer and activator of transcription 3 (STAT3) signaling cascades. Conclusion: Nano-SiO$_2$ has a cytotoxic effect on MDA-MB-231 and Hs578T breast cancer cells via modulation of EGFR signaling cascades.*

Nanoparticles have gathered great scientific interest due to their distinct physical and chemical properties compared to bulk materials (1). Silica nanoparticles (nano-SiO$_2$) are among the most well-known, since SiO$_2$ itself is abundant in the form of quartz, which comprises almost 10% of the crust of earth (2). Nano-SiO$_2$ is used in many industrial applications such as cosmetics, printer toners, and foods (2). There are also several reports which have found that nano-SiO$_2$ is not cytotoxic (3, 4). However, many contradictory studies describe the cytotoxic effect of nano-SiO$_2$ through disruption of endothelial cell function or silicosis (5, 6, 7).

Accordingly, in order to identify the cytotoxicity of nano-SiO$_2$ as well as to validate the potentiality of these nanoparticles as an anticancer agent, we monitored the influence of nano-SiO$_2$ on cancer cell growth, survival, motility, and apoptosis using cultured breast cancer cells.

Materials and Methods

Preparation of nanoparticles. Nano-SiO$_2$ with 30 nm diameter was purchased from Kisker-biotech (Steinfurt, Germany). Stock solution was made by diluting the particles in phosphate-buffered saline (PBS) to 5 mg/ml after sonication at 60 kHz for 20 min. Before immediate use, the stock solution was subjected to sonication under the same conditions.

Cell culture and exposure to nano-SiO$_2$. Human breast carcinoma cell lines MDA-MB-231 and Hs578T were obtained from the American Type Culture Collection (catalog no. CRM-HTB-26 and HTB-126) and maintained in Dulbecco's modified Eagle's medium (DMEM) supplemented with 10% fetal bovine serum (FBS), 100 U/ml penicillin, and 100 mg/ml streptomycin. The cells were maintained in an incubator supplemented with 5% CO$_2$ in humidified air at 37˚C. Each exposure to nano-SiO$_2$ was performed using a mixture of stock solution and normal culture medium and the mixture was prepared immediately before treatment. Culture medium mixed with an equivalent amount of PBS solution was used as a negative control.

Antibodies. Antibodies specific to phosphor-epidermal growth factor receptor (p-EGFR), caspase-3, poly ADP ribose polymerase (PARP), phosphor-signal transducer and activator of transcription 3 (p-STAT3) (Y705), p-STAT3 (S727), phosphor-focal adhesion kinase (p-FAK), FAK, phosphor-cellular sarcoma kinase (p-SRC), and SRC were purchased from Cell Signaling Technology (Beverly, MA, USA). Antibodies against β-tubulin (H-235), cyclin D1 (A-12), cyclin B1 (D-11), p27 (C-19), fibronectin (A-11), survivin (D-8), and STAT3 (H-190) were from Santa Cruz Biotechnology (Santa Cruz, CA, USA). Antibodies for EGFR detection were obtained from Abcam (Cambridge, UK).

Cell proliferation assay. The cells were seeded at 2×10^4 cells per well in 12-well cell culture plates. After 24 h, nano-SiO$_2$ was added at final concentration of 100 μg/ml. Every 24 h for 4 days, the number of cells was counted with a hemocytometer in triplicate.

Correspondence to: Incheol Shin, Department of Life Science, 222, Wangsimni-ro, Seongdong-gu, Seoul, 04763, Republic of Korea. Tel: +82 222202562, Fax: +82 222982562, e-mail: incheol@hanyang.ac.kr

Two-dimensional colony formation assays. The cells were seeded at 100 cells per well in 6-well cell culture plates. Nano-SiO$_2$ was added 3 days post cell-seeding at final concentration of 100 μg/ml. After an additional 5 days, the cells were stained with 0.5% crystal violet for 30 min. After washing with PBS, the number of colonies was counted under an optical microscope. The experiments were performed in triplicate.

MTT assays. Cell viability was measured using the 3-(4,5-dimethylthiazol-2-yl)-2,5-diphenyltetrazolium bromide (MTT) thiazolyl blue assay. Briefly, the cells were seeded in 96-well cell culture plates at 1×10^3 cells per well. After 24 h, nano-SiO$_2$ was added at different concentration and cells were incubated for another 24 or 48 h. MTT (Sigma, St. Louis, MO, USA) was added to each well at a final concentration of 1 mg/ml and incubated for 3 h at 37°C. Formazan was dissolved in dimethyl sulfoxide (DMSO; Sigma), and the optical density was measured at 590 nm using a Multiskan Ex spectrophotometer (Thermo Labsystems, Vantaa, Finland).

Doxorubicin treatment. Doxorubicin was purchased from Calbiochem (Darnstadt, Germany). Before treatment of cells, doxorubicin was initially dissolved in DMSO at the concentration of 10 mM and the stock solution of doxorubicin was diluted and added at final concentration of 10, 50, 100, 500, or 1000 nM to the cells with 100 or 200 μg/ml of nano-SiO$_2$. After 24 h, the viability of the cells was measured with MTT assay.

Cell-cycle analysis by flow cytometry. After exposure to nano-SiO$_2$ at final concentration of 100 μg/ml for 24 h, the cells were fixed in 100% ice-cold methanol for 3 h at −20°C. Fixed cells were incubated in 50 μg/ml propidium iodide (PI) in PBS containing 1 mg/ml RNase for 30 min. Cell cycle analysis was performed using a FACScan flow cytometer (Becton-Dickinson Biosciences, Mountain View, CA, USA) and the data were analyzed using Cell Quest software. The entire experimental procedure was performed independently at least three times.

Cell adhesion assays. The cells were seeded at 5×10^5 cells per well in 12-well cell culture plates with 100 μg/ml nano-SiO$_2$. After 3 h, unattached cells were washed out, and the number of attached cells was estimated with a hemocytometer. The experiments were repeated at least three times independently.

Wound-healing assays. Before seeding, cells were exposed to 100 μg/ml nano-SiO$_2$ for 24 h. The SiO$_2$-treated cells were harvested and re-seeded at 4×10^5 cells in each well of 6-well cell culture plates and incubated for 24 h. After an additional 24 h-incubation in serum-free medium, wounded areas were generated by scraping the culture plates with a pipette tip, and wound closure was observed under a microscope. The ratio of wound-healing (%) was calculated using the following formula: [(width of wounded area at 0 h – width of wounded area at xh)/width of wounded area at 0 h]×100, where x=24, 48, or 72.

Transwell migration and invasion assays. After exposure of cells to 100 μg/ml nano-SiO$_2$ for 24 h, the cells were suspended in serum-free medium and seeded in 8-μm pore size trans-well chambers (Corning, NY, USA). Cells in serum-free medium were transferred into the upper chamber at 1×10^4 cells per chamber, and the lower chambers were filled with serum-containing culture medium. After

18 h, the cells on the bottom surface of the polycarbonate membranes were stained with 0.5% crystal violet, and the number of cells was calculated using an optical microscope. Cell invasion assays were performed with the same method using matrigel-filled upper chambers.

Western blot analysis. Cells exposed to 100 μg/ml nano-SiO$_2$ for 24 h were lysed in a lysis buffer [20 mM Tris–HCl (pH 7.4), 0.1 mM EDTA, 150 mM NaCl, 1% NP-40, 0.1% Triton X-100, 0.1% sodium dodecyl sulfate (SDS), 20 mM NaF, 1 mM Na3VO4, 1×protease inhibitor (Roche, Basel, Switzerland)]. The lysates were boiled with SDS sample buffer, separated on SDS-polyacrylamide gel electrophoresis gels, and blotted onto nitrocellulose membranes (Whatman, Dassel, Germany). After blocking with 5% skim milk for 1 h, the membranes were incubated with appropriate primary antibodies. After 18 h, they were further incubated with horseradish peroxidase-conjugated secondary antibodies. Protein bands were visualized with the Dyne ECL STAR Western Blotting Detection Kit (Dyne Bio, Seongnam, Korea).

Gefitinib treatment. Gefitinib was obtained from Biaffin GmbH (Kassel, Germany). Before treatment of cells, stock solution of gefitinib was initially made by dissolving in DMSO at 10 μM. The stock solution was further diluted in cell culture medium at a final concentration of 10 nM and added to breast cancer cells. Culture medium mixed with an equivalent amount of DMSO was used as a negative control.

Quantitative real-time polymerase chain reaction (qPCR). After exposure to 100 μg/ml nano-SiO$_2$ for 24 h, RNA was isolated from the cells using Trizol reagent (MRC, Cincinnati, OH, USA). Quantitative real-time PCR was performed with a SYBR FAST qPCR kit (KAPA) in a Thermal Cycler Dice (Takara, Otsu, Shiga, Japan), according to the manufacturer's instructions. The C(t) value was normalized using glyceraldehyde 3-phosphate dehydrogenase (*GAPDH*). Primers were: *GAPDH*: forward: 5'-TCA GTG GTG GAC CTG ACC TGA CC-3', reverse: 5'-TGC TGT AGC CAA ATT CGT TGT CAT ACC-3'; fibronectin: forward: 5'-GTT GTT ACC GTG GGC AAC TCT GTC-3', reverse: 5'-AAA GCC TAA GCA CTG GCA CAA CAG-3'; survivin: forward: 5'-CTT GGA GGG CTG CGC CTG CAC CC-3', reverse: 5'- CTG GCT CCC AGC CTT CCA GCT CCT TG-3'; FAK: forward: 5'-ATG GCA GCT GCT TAC CTT GAC CCC A-3', reverse: 5'-TGC ATT GCC CCG CAT CTC CCA-3'.

Covalent crosslinking. After the cells were exposed to 100 μg/ml nano-SiO$_2$ for 24 h, 1 mM bis(sulfosuccinimidyl)suberate (BS3) (Thermo Scientific, Rockford, IL, USA) crosslinking reagent was added for 30 min at 4°C. Crosslinking reactions were terminated by 10 mM Tris (pH 7.5) treatment for 5 min. The detection of dimerized EGFR was monitored by western blots using antibody to EGFR.

Results

Nano-SiO$_2$ has cytotoxic effects on breast cancer cells. To investigate the cytotoxic effect of nano-SiO$_2$ on breast cancer cells, we first measured the growth of human breast cancer cell lines MDA-MB-231 and Hs578T with and without nano-SiO$_2$. As shown in Figure 1A, cell proliferation significantly decreased upon exposure to nano-SiO$_2$. To confirm the anti-

proliferative effect of these nanoparticles, we further measured the number of colonies formed (Figure 1B). Compared to control cells, the number of colonies decreased significantly following SiO$_2$ treatment. Next, we performed MTT assays to examine the effect of nano-SiO$_2$ on cancer cell viability (Figure 1C). Upon 24-h exposure to nano-SiO$_2$ at concentrations above 50 μg/ml, cell viability decreased slightly in both cell lines. After 48 h of treatment, there was a significant reduction in cell viability of MDA-MB-231 for all dosages of nano-SiO$_2$ and of Hs578T cells for dosages over 100 μg/ml. To examine the effect of nano-SiO$_2$ on doxorubicin-induced cancer cell death, we next monitored the combined effect of the anticancer drug doxorubicin and nanoparticles on breast cancer cells (Figure. 1D). Co-treatment with nano-SiO$_2$ additively increased doxorubicin toxicity. However, there was no significant additional decrease of cell viability when SiO$_2$ concentration was increased two-fold from 100 μg/ml to 200 μg/ml, except in the case of 1000 nM doxorubicin-treated Hs578T cells.

Nano-SiO$_2$ alters cell-cycle distribution and induces apoptosis of breast cancer cells. To identify the mechanism responsible for the decrease in cancer cell viability, we further analyzed cell-cycle profiles (Figures 2A). There was a significant increase in the sub-G$_1$ fractions in nano-SiO$_2$-exposed cancer cells, indicating that nano-SiO$_2$ activated apoptotic signals. Therefore, we monitored the proteins related to apoptosis after exposure to nano-SiO$_2$ (Figure 2B). Activation of caspase-3 through its cleavage and subsequent induction of PARP cleavage are hallmarks of cellular apoptosis (8). Alteration of protein levels of cyclin B1, cyclin D1, p27 and survivin are also considered common phenomena of apoptosis (9-12). Therefore, we investigated the amount of these proteins after exposure of breast cancer cells to nano-SiO$_2$. We found that the cleaved form of PARP and caspase-3 increased and the amount of cyclin D1, cyclin B1 and survivin decreased significantly upon nano-SiO$_2$ treatment, while the p27 level remained unchanged. These results indicate that nano-SiO$_2$ reduces cancer cell viability through induction of apoptosis of breast cancer cells.

Nano-SiO$_2$ disturbs cancer cell adhesion and migration. In addition to the harmful effects of nano-SiO$_2$ on cell growth, the disturbance of cell motility by nanoparticles has been reported (13). Therefore, we also investigated whether nano-SiO$_2$ disturbs the cellular motility of breast cancer cells. We found that treatment with nano-SiO$_2$ disturbed adherence of breast cancer cells to the surface of cell culture plates (Figure 3A). Next, we monitored the rate of wound-healing (Figure 3B). When the cancer cells were exposed to nano-SiO$_2$, cellular motility was severely impaired. Together, the results in Figure 3C and D provide evidence that the migratory and invasive abilities of the cancer cells were disturbed by nano-SiO$_2$.

Nano-SiO$_2$ exerts cancer cell cytotoxicity via modulation of EGFR signaling cascades. EGFR is a receptor tyrosine kinase overexpressed in many breast carcinomas and has roles in cell survival, growth, migration, and invasion (14-18). Therefore, we examined whether exposure to nano-SiO$_2$ affects EGFR signaling (Figure 4A). Among the various signaling cascades, we focused on the EGFR/c-SRC/STAT3 signaling cascade (19, 20). STAT3 is activated by c-SRC_mediated phosphorylation (21, 22) and is a known transcription factor for cyclin B1, cyclin D1 and survivin (23-25). We found that the phosphorylation of EGFR decreased after nano-SiO$_2$ exposure, without any alteration of total EGFR. In addition, phosphorylation of c-SRC was reduced, followed by a decrease of STAT3 phosphorylation. We also confirmed the repression of the STAT3 targets, including cyclin B1, cyclin D and survivin. Additionally, we monitored the protein levels of FAK and fibronectin, which play important roles in cellular motility (26-28). There were significant decreases in the total amounts of fibronectin and FAK, as well as of phosphorylated FAK. We further examined the transcript level of SiO$_2$-treated cancer cells, and found down-regulation of *FAK*, fibronectin, and survivin expression to be induced by exposure to nanoparticles (Figure 4B). To determine whether these phenomena occurred *via* disturbance of EGFR downstream signaling cascades, we employed a parallel set of experiments using gefitinib, a specific inhibitor of EGFR (29). We found a similar shift of molecular patterns after gefitinib treatment (Figure 4A).

Based on these findings, we next hypothesized that the decrease of EGFR phosphorylation occurs through the disturbance of EGFR dimerization. EGFR activates its downstream signaling *via* formation of homo- and hetero-dimers with avian erythroblastosis oncogene B (ERBB) family proteins after ligand binding (18). Therefore, we investigated whether nano-SiO$_2$ exposure disrupted the formation of EGFR dimers (Figure 4C). In both cancer cell lines, the amount of dimerized EGFR significantly decreased on exposure to nano-SiO$_2$, indicating that nano-SiO$_2$ disturbs EGFR dimerization.

Discussion

Nano-SiO$_2$ is one of the most well-known nanoparticles and has been applied in many industrial fields such as cosmetics and drugs (2). We monitored the cytotoxicity of nano-SiO$_2$ in breast cancer cell lines. We found a disturbance in cancer cell growth (Figures 1A and B), viability (Figure 1C), and sensitivity toward doxorubicin induced by nano-SiO$_2$ (Figure 1D). Furthermore, the cancer cells exposed to nano-SiO$_2$ exhibited increased apoptosis (Figure 2), and changes in several markers of apoptosis (Figure 2B).
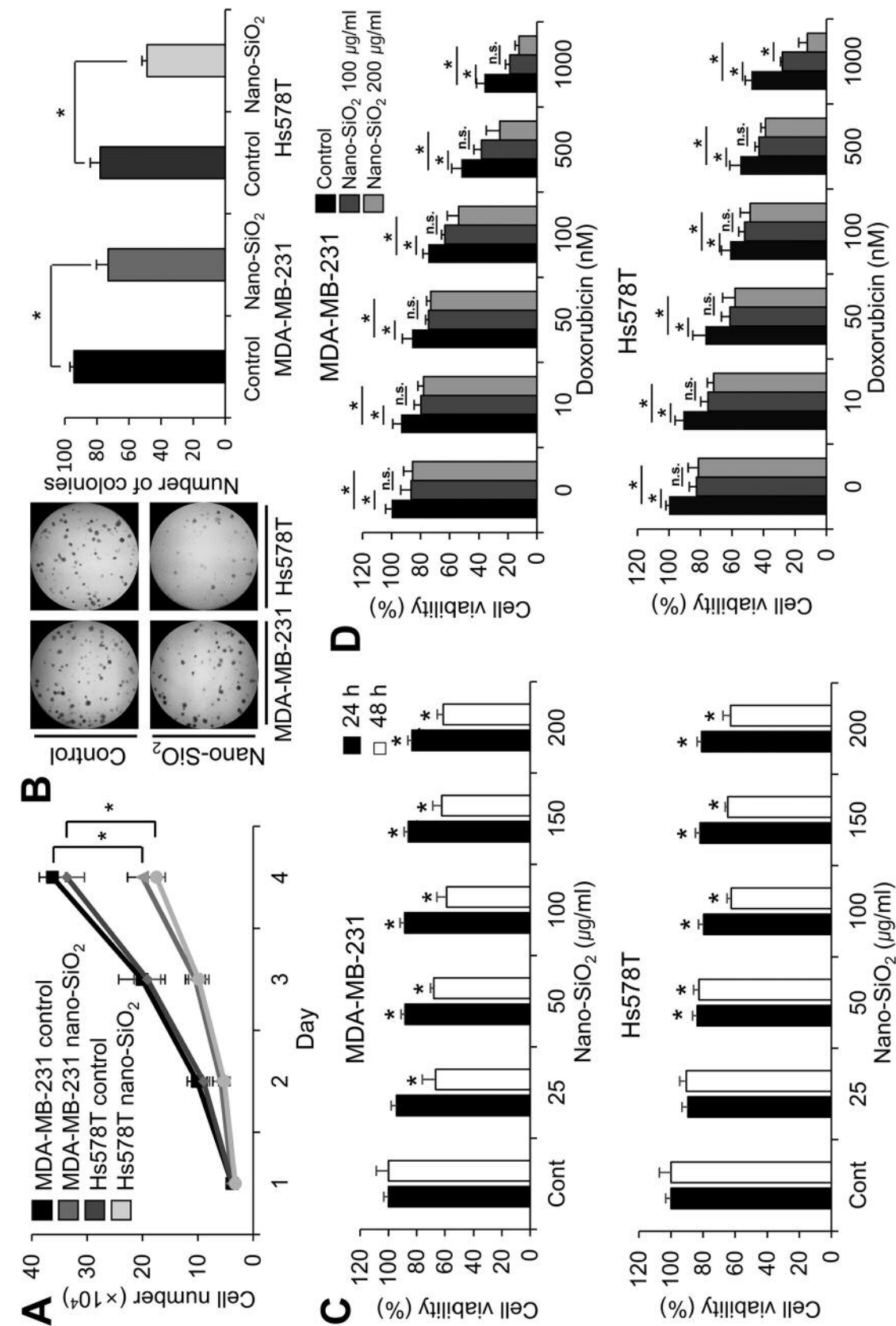
Figure 1. Cytotoxicity of nano-SiO₂ towards human breast cancer cells. The cells were seeded in 12-well plates and were exposed to 100 μg/ml nano-SiO₂. The cells were counted for 4 days. B: Nano-SiO₂ affected the colony-forming ability of the cancer cells. The cells were seeded in 6-well plates and 100 μg/ml nano-SiO₂ were treated after 3 days. After another 5 days, the number of colonies were counted under a microscope. C: Nano-SiO₂ reduced cell viability of the cancer cells. The cells were seeded, incubated with nano-StO₂ and cell viability was monitored by MTT assay. D: Nano-SiO₂ sensitized breast cancer cells to doxorubicin-induced cytotoxicity. Doxorubicin was added at a concentration of 10, 50, 100, 500, or 1000 nM to the cells, and where indicated, 100 or 200 μg/ml of nano-SiO₂ were also added. Each bar represents the mean±SD of three independent experiments. *Significantly different at p<0.05.

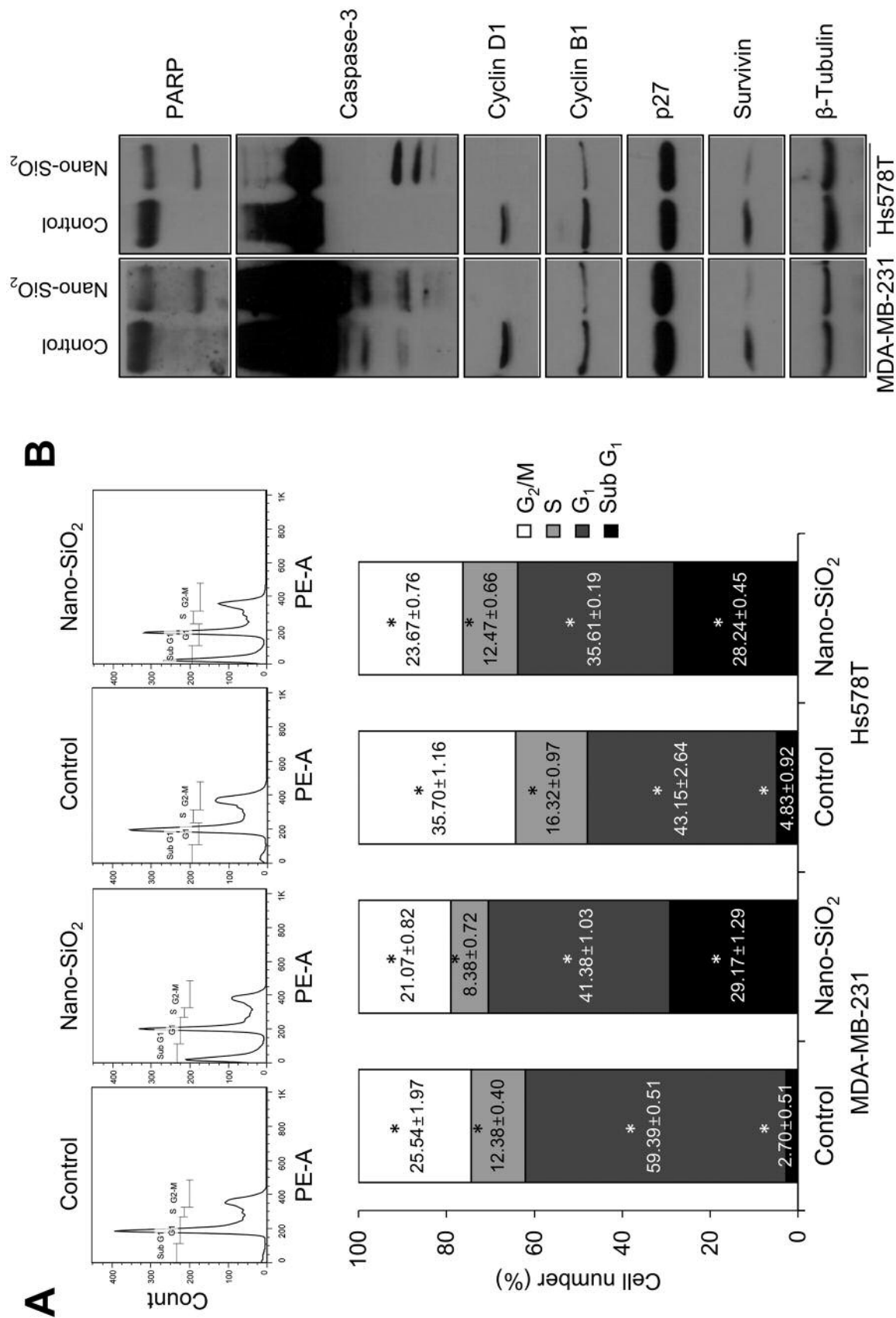Figure 2. *Effects of nano-SiO$_2$ on cell-cycle alteration and apoptosis in breast cancer cells. A: Cell-cycle alteration and apoptosis in breast cancer cells was detected after nano-SiO$_2$ treatment. The cells were treated with 100 μg/ml nano-SiO$_2$. After 24 h, the cells were fixed and cell-cycle distribution was analyzed. B: Proteins related to apoptosis were examined by western blot. Each bar represents the mean±SD of three independent experiments. *Significantly different at p<0.05.*
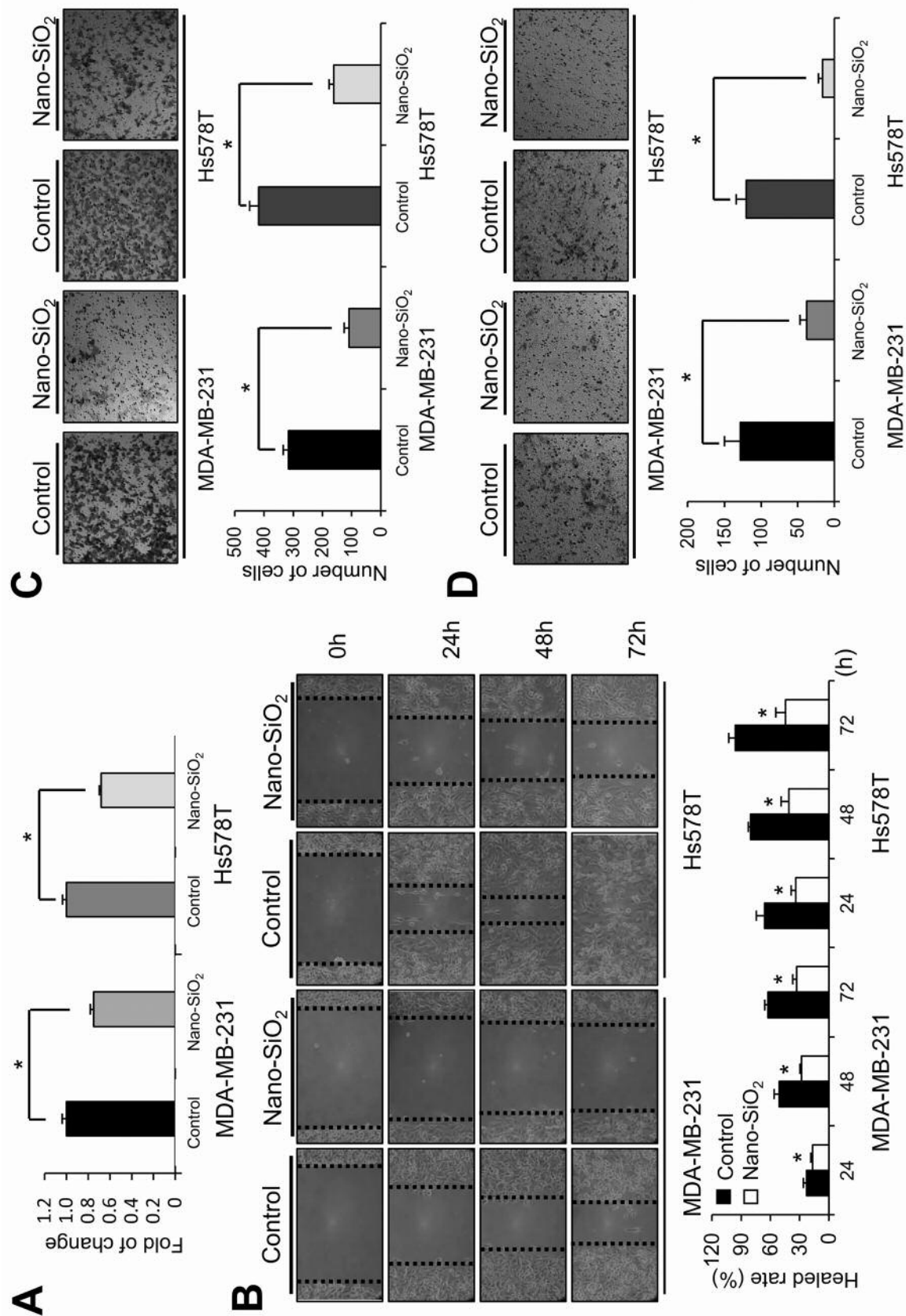
Figure 3. Effects of nano-SiO₂ on cancer cell adhesion and motility. A: Nano-SiO₂ disturbed cell adhesion of breast cancer cells. The cells were seeded with 100 μg/ml nano-SiO₂, and after 3 h, the number of attached cells was counted. B: For wound-healing assay, control and SiO₂-treated cancer cells were seeded and vertical wounds were created. The widths of the wounded areas were measured under a microscope. C: Nano-SiO₂ inhibited cancer cell migration. After exposure to 100 μg/ml nano-SiO₂, the cancer cells were seeded in trans-well chambers and migrated cells were counted. D: Invasive properties of cancer cells were examined using transwell chambers coated with matrigel. Cancer cells that invaded through the matrigel were stained and counted. Each bar represents the mean±SD of three independent experiment. *Significantly different at p<0.05.

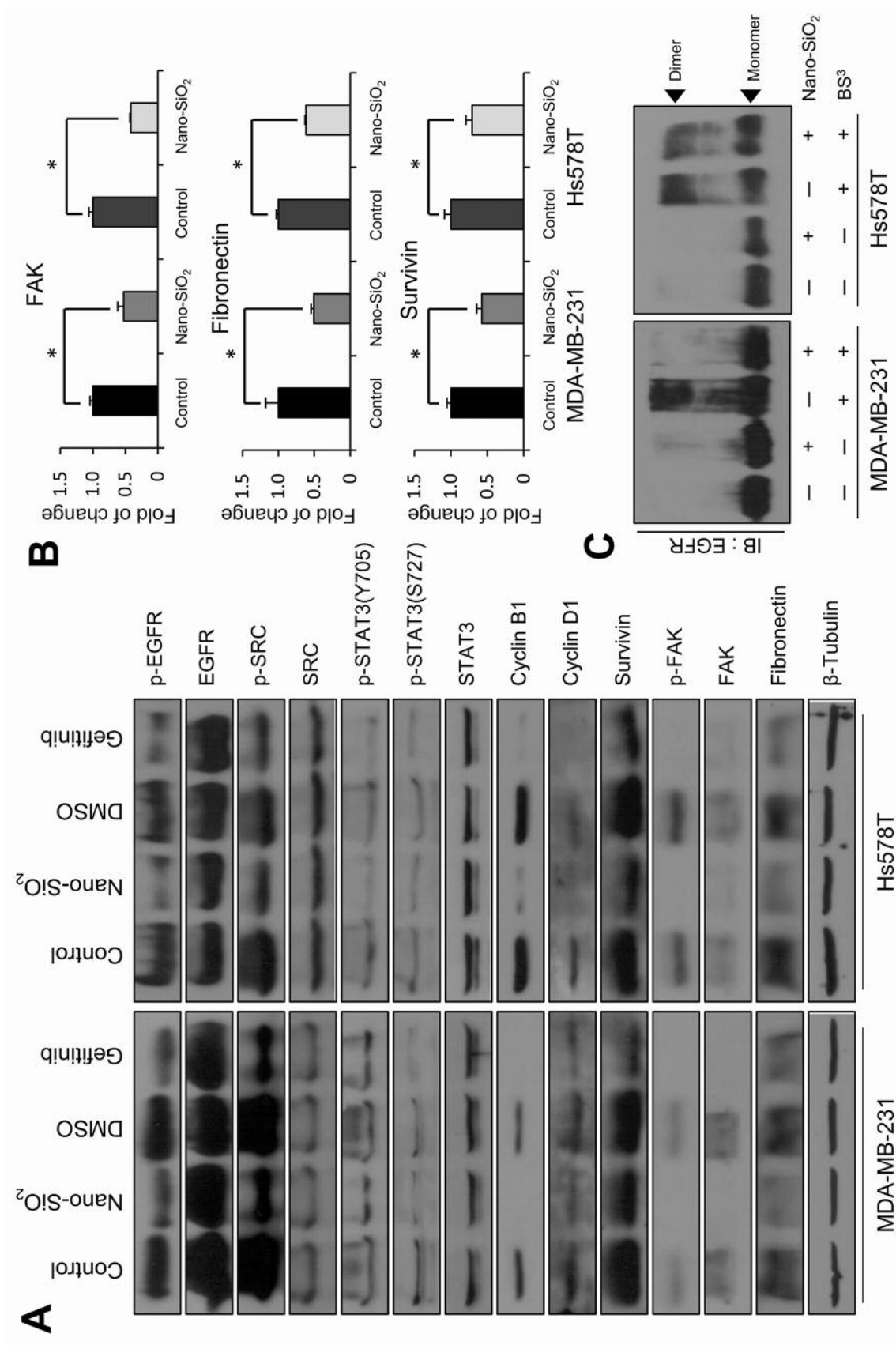Figure 4. *Nano-SiO$_2$ induced modulation of epidermal growth factor receptor (EGFR) signaling cascades. A: Down-regulation of the EGFR signaling pathway in breast cancer cells after nano-SiO$_2$ treatment was monitored. After incubation with 100 μg/ml nano-SiO$_2$, the cells were subjected to western blotting. Gefitinib-treated cells were used as positive controls for EGFR inhibition. Treatment of gefitinib was performed at a final concentration of 10 nM. Culture medium mixed with dimethyl surfoxide (DMSO) was used as a negative control. B: mRNA levels of focal adhesion kinase (FAK), fibronectin and survivin were measured after nano-SiO$_2$ treatment via quantitative real-time polymerase chain reaction. C: The effect of nano-SiO$_2$ on EGFR dimerization was monitored. After nano-SiO$_2$ treatment at final concentration of 100 μg/ml, the cancer cells were incubated with BS3 cross-linking reagents and the amount of dimerized EGFR was analyzed. *Significantly different at p<0.05.*

Many researchers studying the cytotoxicity of nanoparticles have focused on the acute-phase cytotoxicity of them based on cell viability or gene expression. However, the impact of nanoparticles on cell viability is only part of the picture, since nanoparticles can affect other aspects of cellular phenomena such as cellular movement (13). Accordingly, we investigated the motility of cancer cells as well as cell growth, survival, and apoptosis after nano-SiO$_2$ treatment. We found that nano-SiO$_2$ disrupted cellular adhesion, migration, and invasion, and we further attempted to elucidate the mechanism(s) responsible for those phenomena.

Since EGFR is important in cancer cell migration and invasion as well as cell survival and growth (16-18), we analyzed a possible modulation of the EGFR signaling cascade by nano-SiO$_2$. We found that nano-SiO$_2$ treatment down-regulated EGFR, c-SRC, and STAT3 phosphorylation. In addition, expression of FAK, fibronectin, cyclins, and survivin decreased upon the nanoparticle through western blot and qRT-PCR. Although we do not have a mechanistic explanation for the transcriptional down-regulation of these genes, these results are in accordance with previous findings that blockage of EGFR signaling leads to down-regulation of these genes (30-32). Accordingly, we further detected the decreased dimerization of EGFR by nano-SiO$_2$ (Figure 4C). However, given that EGFR is a member of the ERBB family and can also form heterodimers with other ERBB family members (18), it is possible that the EGFR blot for dimer shown in Figure 4C may contain EGFR heterodimers as well as homodimers.

We used gefitinib as an inhibitor of EGFR signaling, and it also down-regulated EGFR downstream. However, considering that gefitinib blocks the tyrosine kinase domain of EGFR, gefitinib itself might not be regarded as a perfect positive control for disruption of EGFR dimerization. Furthermore, some reports demonstrate that it plays a role in EGFR dimerization *via* formation of inactive EGFR dimers or blockage of interactions between EGFR and its ligand EGF, even though the final consequence is still blockage of EGFR downstream signaling (33, 34). Therefore, other methods for monitoring EGFR dimerization may be required in order to fully understand the effect of nano-SiO$_2$ on EGFR dimerization.

We found that nano-SiO$_2$ influenced activation of EGFR through interruption of its dimerization and led to down-regulation of signaling molecules, followed by adverse effects on cancer cell-proliferation and migration. Our results imply that disturbance of cell surface receptor functioning might be another reason for the cytotoxic effects of nanoparticles, although some reports implicate the generation of reactive oxygen species as a potential mechanism responsible for nano-SiO$_2$-induced cytotoxicity (6, 35). In this regard, we propose that cytotoxic effect of nano-SiO$_2$ in breast cancer cells involves the disturbance of EGFR dimerization and subsequent modulation of downstream signaling cascades.

Acknowledgements

References

1 Hewakuruppu YL, Dombrovsky LA, Chen C, Timchenko V, Jiang X, Baek S and Taylor RA: Plasmonic "pump-probe" method to study semi-transparent nanofluids. Appl Opt *52*: 6041-6050, 2013.

2 Flörke OW, Graetsch HA, Brunk F, Benda L, Paschen S, Bergna HE, Roberts WO, Welsh WA, Libanati C, Ettlinger M, Kerner D, Maier M, Meon W, Schmoll R, Gies H and Schiffmann D: Silica. *In*: Ullmann's Encyclopedia of Industrial Chemistry: Wiley-VCH Verlag GmbH & Co. KGaA, 2000.

3 Li Z, Barnes JC, Bosoy A, Stoddart JF and Zink JI: Mesoporous silica nanoparticles in biomedical applications. Chem Soc Rev *41*: 2590-2605, 2012.

4 Barnes CA, Elsaesser A, Arkusz J, Smok A, Palus J, Lesniak A, Salvati A, Hanrahan JP, Jong WH, Dziubaltowska E, Stepnik M, Rydzynski K, McKerr G, Lynch I, Dawson KA and Howard CV: Reproducible comet assay of amorphous silica nanoparticles detects no genotoxicity. Nano Lett *8*: 3069-3074, 2008.

5 Rimal B, Greenberg AK and Rom WN: Basic pathogenetic mechanisms in silicosis: current understanding. Curr Opin Pulm Med *11*: 169-173, 2005.

6 Liu X and Sun J: Endothelial cells dysfunction induced by silica nanoparticles through oxidative stress *via* JNK/P53 and NF-kappaB pathways. Biomaterials *31*: 8198-8209, 2010.

7 Choi M, Cho WS, Han BS, Cho M, Kim SY, Yi JY, Ahn B, Kim SH and Jeong J: Transient pulmonary fibrogenic effect induced by intratracheal instillation of ultrafine amorphous silica in A/J mice. Toxicol Lett *182*: 97-101, 2008.

8 Simbulan-Rosenthal CM, Rosenthal DS, Iyer S, Boulares H and Smulson ME: Involvement of PARP and poly(ADP-ribosyl)ation in the early stages of apoptosis and DNA replication. Mol Cell Biochem *193*: 137-148, 1999.

9 Yuan J, Yan R, Kramer A, Eckerdt F, Roller M, Kaufmann M and Strebhardt K: Cyclin B1 depletion inhibits proliferation and induces apoptosis in human tumor cells. Oncogene *23*: 5843-5852, 2004.

10 Sauter ER, Nesbit M, Litwin S, Klein-Szanto AJ, Cheffetz S and Herlyn M: Antisense cyclin D1 induces apoptosis and tumor shrinkage in human squamous carcinomas. Cancer Res *59*: 4876-4881, 1999.

11 Rodel F, Hoffmann J, Grabenbauer GG, Papadopoulos T, Weiss C, Gunther K, Schick C, Sauer R and Rodel C: High survivin expression is associated with reduced apoptosis in rectal cancer and may predict disease-free survival after preoperative radiochemotherapy and surgical resection. Strahlenther Onkol *178*: 426-435, 2002.

12 Katayose Y, Kim M, Rakkar AN, Li Z, Cowan KH and Seth P: Promoting apoptosis: a novel activity associated with the cyclin-dependent kinase inhibitor p27. Cancer Res *57*: 5441-5445, 1997.

13 Zhang Y, Hu L, Yu D and Gao C: Influence of silica particle internalization on adhesion and migration of human dermal fibroblasts. Biomaterials *31*: 8465-8474, 2010.

14 Subik K, Lee JF, Baxter L, Strzepek T, Costello D, Crowley P, Xing L, Hung MC, Bonfiglio T, Hicks DG and Tang P: The expression patterns of ER, PR, HER2, CK5/6, EGFR, Ki-67 and AR by immunohistochemical analysis in breast cancer cell lines. Breast Cancer *4*: 35-41, 2010.

15 Rusnak DW, Alligood KJ, Mullin RJ, Spehar GM, Arenas-Elliott C, Martin AM, Degenhardt Y, Rudolph SK, Haws TF Jr., Hudson-Curtis BL and Gilmer TM: Assessment of epidermal growth factor receptor (EGFR, ERBB1) and HER2 (ERBB2) protein expression levels and response to lapatinib (Tykerb, GW572016) in an expanded panel of human normal and tumour cell lines. Cell Prolif *40*: 580-594, 2007.

16 Price JT, Tiganis T, Agarwal A, Djakiew D and Thompson EW: Epidermal growth factor promotes MDA-MB-231 breast cancer cell migration through a phosphatidylinositol 3'-kinase and phospholipase C-dependent mechanism. Cancer Res *59*: 5475-5478, 1999.

17 Park EJ, Min HY, Chung HJ, Hong JY, Kang YJ, Hung TM, Youn UJ, Kim YS, Bae K, Kang SS and Lee SK: Down-regulation of c-SRC/EGFR-mediated signaling activation is involved in the honokiol-induced cell-cycle arrest and apoptosis in MDA-MB-231 human breast cancer cells. Cancer Lett *277*: 133-140, 2009.

18 Masuda H, Zhang D, Bartholomeusz C, Doihara H, Hortobagyi GN and Ueno NT: Role of epidermal growth factor receptor in breast cancer. Breast Cancer Res Treat *136*: 331-345, 2012.

19 Grandis JR, Drenning SD, Chakraborty A, Zhou MY, Zeng Q, Pitt AS and Tweardy DJ: Requirement of STAT3 but not STAT1 activation for epidermal growth factor receptor- mediated cell growth *in vitro*. J Clin Invest *102*: 1385-1392, 1998.

20 Cao D, Tal TL, Graves LM, Gilmour I, Linak W, Reed W, Bromberg PA and Samet JM: Diesel exhaust particulate-induced activation of STAT3 requires activities of EGFR and SRC in airway epithelial cells. Am J Physiol Lung Cell Mol Physiol *292*: L422-429, 2007.

21 Olayioye MA, Beuvink I, Horsch K, Daly JM and Hynes NE: ERBB receptor-induced activation of STAT transcription factors is mediated by SRC tyrosine kinases. J Biol Chem *274*: 17209-17218, 1999.

22 Irwin ME, Bohin N and Boerner JL: SRC family kinases mediate epidermal growth factor receptor signaling from lipid rafts in breast cancer cells. Cancer Biol Ther *12*: 718-726, 2011.

23 Liu T, Peng H, Zhang M, Deng Y and Wu Z: Cucurbitacin B, a small molecule inhibitor of the STAT3 signaling pathway, enhances the chemosensitivity of laryngeal squamous cell carcinoma cells to cisplatin. Eur J Pharmacol *641*: 15-22, 2010.

24 Leslie K, Lang C, Devgan G, Azare J, Berishaj M, Gerald W, Kim YB, Paz K, Darnell JE, Albanese C, Sakamaki T, Pestell R and Bromberg J: Cyclin D1 is transcriptionally regulated by and required for transformation by activated signal transducer and activator of transcription 3. Cancer Res *66*: 2544-2552, 2006.

25 Gritsko T, Williams A, Turkson J, Kaneko S, Bowman T, Huang M, Nam S, Eweis I, Diaz N, Sullivan D, Yoder S, Enkemann S, Eschrich S, Lee JH, Beam CA, Cheng J, Minton S, Muro-Cacho CA and Jove R: Persistent activation of STAT3 signaling induces survivin gene expression and confers resistance to apoptosis in human breast cancer cells. Clin Cancer Res *12*: 11-19, 2006.

26 Sieg DJ, Hauck CR and Schlaepfer DD: Required role of focal adhesion kinase (FAK) for integrin-stimulated cell migration. J Cell Sci *112(Pt 16)*: 2677-2691, 1999.

27 Meng XN, Jin Y, Yu Y, Bai J, Liu GY, Zhu J, Zhao YZ, Wang Z, Chen F, Lee KY and Fu SB: Characterisation of fibronectin-mediated FAK signalling pathways in lung cancer cell migration and invasion. Br J Cancer *101*: 327-334, 2009.

28 Ioachim E, Charchanti A, Briasoulis E, Karavasilis V, Tsanou H, Arvanitis DL, Agnantis NJ and Pavlidis N: Immunohistochemical expression of extracellular matrix components tenascin, fibronectin, collagen type IV and laminin in breast cancer: their prognostic value and role in tumour invasion and progression. Eur J Cancer *38*: 2362-2370, 2002.

29 Herbst RS, Fukuoka M and Baselga J: Gefitinib–a novel targeted approach to treating cancer. Nat Rev Cancer *4*: 956-965, 2004.

30 Li S, Huang X, Zhang D, Huang Q, Pei G, Wang L, Jiang W, Hu Q, Tan R and Hua ZC: Requirement of PEA3 for transcriptional activation of FAK gene in tumor metastasis. PLoS One *8*: e79336, 2013.

31 Uchiyama-Tanaka Y, Matsubara H, Mori Y, Kosaki A, Kishimoto N, Amano K, Higashiyama S and Iwasaka T: Involvement of HB-EGF and EGF receptor transactivation in TGF-beta-mediated fibronectin expression in mesangial cells. Kidney Int *62*: 799-808, 2002.

32 Wang Q and Greene MI: EGFR enhances survivin expression through the phosphoinositide 3 (PI-3) kinase signaling pathway. Exp Mol Pathol *79*: 100-107, 2005.

33 Bjorkelund H, Gedda L, Barta P, Malmqvist M and Andersson K: Gefitinib induces epidermal growth factor receptor dimers which alters the interaction characteristics with (1)(2)(5)I-EGF. PLoS One *6*: e24739, 2011.

34 Favoni RE, Pattarozzi A, Lo Casto M, Barbieri F, Gatti M, Paleari L, Bajetto A, Porcile C, Gaudino G, Mutti L, Corte G and Florio T: Gefitinib targets EGFR dimerization and ERK1/2 phosphorylation to inhibit pleural mesothelioma cell proliferation. Curr Cancer Drug Targets *10*: 176-191, 2010.

35 Park EJ and Park K: Oxidative stress and pro-inflammatory responses induced by silica nanoparticles *in vivo* and *in vitro*. Toxicol Lett *184*: 18-25, 2009.